Experiments in Fluids 12, 17–22 (1991)

Experiments in Fluids

A crossed hot-wire technique for complex turbulent flows

A. D. Cutler* and **P. Bradshaw**

Department of Aeronautics Imperial College of Science and Technology, London SW7 2BY, GB

Abstract. This paper describes a crossed hot-wire technique for the measurement of all components of mean velocity, Reynolds stresses, and triple products in a complex turbulent flow. The accuracy of various assumptions usually implicit in the use of crossed hot-wire anemometers is examined. It is shown that significant errors can result in flow with gradients in mean velocity or Reynolds stress, but that a first order correction for these errors can be made using available data. It is also shown how corrections can be made for high turbulence levels using available data.

1 Introduction

Hot-wire anemometry continues to be the technique of choice for measurement of turbulence quantities in non-hostile flow environments, provided the relative levels of turbulence fluctuations are not too large. Hot-wire techniques have been used with great success for many years in relatively simple flow situations, such as two-dimensional boundary layers and shear layers. In order to satisfy the demands of computational fluid dynamics, experimental data are required in more complex flows, such as three-dimensional boundary layers and vortical flows. Modelers typically require, as a minimum, distributions of mean velocity and Reynolds stresses for the development and validation of codes.

One of the most common techniques for making such measurements uses the crossed hot-wire anemometer. Typically, the probe must be aligned with the mean flow direction. Measurements are then made of the two mean velocity components, the three Reynolds stresses, and the four triple products which lie in the plane of the wires. If the procedure is repeated three more times, after rolling the probe about its axis to positions 45°, 90°, and 135° with respect to the start, the results can be combined to obtain all three mean velocity components, six Reynolds stresses, and the ten triple products.

When using a crossed hot-wire anemometer to make measurements in a turbulent flow a number of simplifying assumptions usually have to be made. The instantaneous velocity is assumed uniform over the volume defined by the active portion of the two wires. Hirota et al. (1988) investigated the accuracy of this assumption by comparison of the results from a pair of crossed hot-wire probes, one of which was the mirror image of the other. They showed that significant errors could be produced by gradients, but that the error could be reduced by combining the results from the two probes. Another common assumption is that the velocity fluctuations are a small fraction of the mean velocity. This leads to substantial errors in flows where the turbulence intensities exceed about 20% (Bruun, 1972). Techniques are described for estimating, and correcting, both types of errors.

* Corresponding author.
Current address: The George Washington University JIAFS. M.S. 269, NASA, Hampton, VA 23665, USA

2 Analysis

In the discussion below we shall use three sets of coordinates (Fig. 1 and 2): *tunnel axes* in which the final results are to be presented; *probe axes*, with x_p along the probe roll axis and y_p and z_p perpendicular to this; and *wire axes*, with x_w the same as x_p but with y_w and z_w parallel and normal to the plane of the wires (the probe axes and the wire axes are coincident at zero roll angle). The wires are a distance Δ apart. It is assumed that a cosine cooling law is applicable, so that the heat transfer from a given wire of the probe is dependent only on the component of velocity normal to the wire. This is a good assumption provided that the wire angle used is an effective (best fit) wire angle, determined by a yaw calibration (Bradshaw, 1971), rather than the geometric angle. For the sake of the present discussion it is assumed that the wire angles relative to the roll axis are $\pm 45°$: it would be a simple matter to extend the analysis to other angles. Thus, the heat transfer from wire 1 of the probe is a function of $\sqrt{\frac{1}{2}(u_w+v_w)^2+w_w^2}$ at $z_w=-\Delta/2$, while the heat transfer from wire 2 is a function of $\sqrt{\frac{1}{2}(u_w-v_w)^2+w_w^2}$ at $z_w=\Delta/2$. These effective cooling velocities can be detemined from the hot-wire voltages by calibration.

Assumptions usually made in the implementation of the crossed hot-wire technique include: (i) the variation of in-

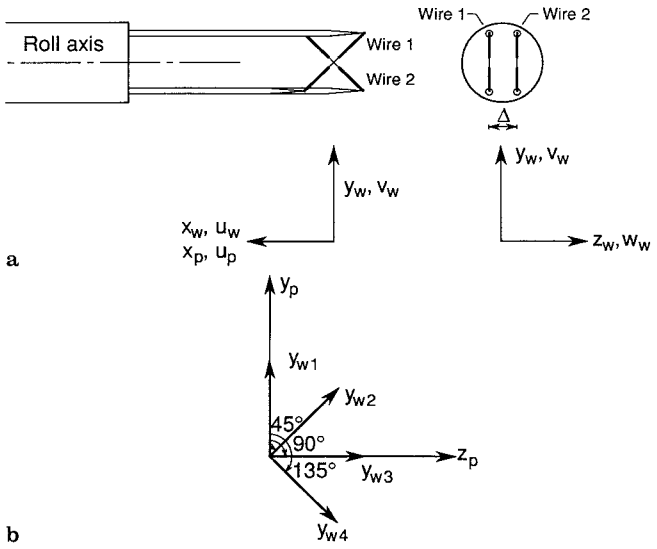

Fig. 1 a and b. Wire (suffix w) axes and probe (suffix p) axes; **a** wire axes; **b** the y_p, z_p plane, showing probe axes and the four positions of the wires

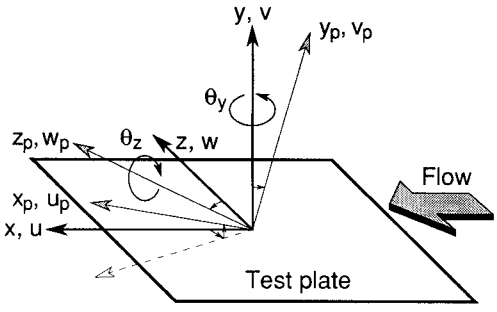

Fig. 2. The relation between tunnel axes and probe (suffix p) axes

stantaneous velocity between the two wires is negligible; (ii) the variation of instantaneous velocity along the active region of a given wire is negligible; (iii) the mean velocity vector is roughly aligned with the axis of the probe; and (iv) velocity fluctuations are a small fraction of the mean velocity. The effects of variation of velocity along a given wire are of a higher order than the effects of wire-to-wire variations, so need not be considered in the present discussion. Assumptions (iii) and (iv) allow us to set $w_w=0$ in the equations for the effective cooling velocity. It is then a simple matter to solve for u_w and v_w in terms of the effective cooling velocities for wire 1 and wire 2 of the probe.

The instantaneous velocity pairs u_w and v_w are sampled, and the mean velocities, the Reynolds stresses, and the triple products are formed. Measurements are obtained in four roll positions as shown in Fig. 1 (b), denoted by suffixes 1 to 4 in the equations. The results are then combined to give the full set of velocity components, Reynolds stresses, and triple products in probe axes:

$$\overline{u_p}=\tfrac{1}{4}(\overline{u_{w1}}+\overline{u_{w2}}+\overline{u_{w3}}+\overline{u_{w4}}) \tag{1}$$
$$\overline{v_p}=\overline{v_{w1}}$$
$$\overline{w_p}=\overline{v_{w3}}$$
$$\overline{u_p'^2}=\tfrac{1}{4}(\overline{u_{w1}'^2}+\overline{u_{w2}'^2}+\overline{u_{w3}'^2}+\overline{u_{w4}'^2})$$
$$\overline{v_p'^2}=\overline{v_{w1}'^2}$$
$$\overline{w_p'^2}=\overline{v_{w3}'^2}$$
$$\overline{u_p' v_p'}=\overline{u_{w1}' v_{w1}'}$$
$$\overline{u_p' w_p'}=\overline{u_{w3}' v_{w3}'}$$
$$\overline{v_p' w_p'}=\tfrac{1}{2}(\overline{v_{w2}'^2}-\overline{v_{w4}'^2})$$
$$\overline{u_p'^3}=\tfrac{1}{4}(\overline{u_{w1}'^3}+\overline{u_{w2}'^3}+\overline{u_{w3}'^3}+\overline{u_{w4}'^3})$$
$$\overline{v_p'^3}=\overline{v_{w1}'^3}$$
$$\overline{w_p'^3}=\overline{v_{w3}'^3}$$
$$\overline{u_p'^2 v_p'}=\overline{u_{w1}'^2 v_{w1}'}$$
$$\overline{u_p'^2 w_p'}=\overline{u_{w3}'^2 v_{w3}'}$$
$$\overline{u_p' v_p'^2}=\overline{u_{w1}' v_{w1}'^2}$$
$$\overline{u_p' w_p'^2}=\overline{u_{w3}' v_{w3}'^2}$$
$$\overline{v_p'^2 w_p'}=\tfrac{1}{3}(\sqrt{2}(\overline{v_{w2}'^3}+\overline{v_{w4}'^3})-\overline{v_{w3}'^3})$$
$$\overline{v_p' w_p'^2}=\tfrac{1}{3}(\sqrt{2}(\overline{v_{w2}'^3}-\overline{v_{w4}'^3})-\overline{v_{w1}'^3})$$
$$\overline{u_p' v_p' w_p'}=\tfrac{1}{2}(\overline{u_{w2}' v_{w2}'^2}-\overline{u_{w4}' v_{w4}'^2})$$

The equivalence of the left and the right hand side of Eq. (1) is easily demonstrated by transforming the terms on the right hand side from wire to probe axes. This is done with the following equations, expressed in tensor notation (i.e. repeated indices are summed from 1 to 3, where $x_1=x$, $x_2=y$, $x_3=z$, $u_1=u$, $u_2=v$, $u_3=w$):

$$\overline{(u_i)_w}=a_{ij}\,\overline{(u_j)_p} \tag{2}$$
$$\overline{(u_i)_w'(u_j)_w'}=a_{ik}\,a_{jl}\overline{(u_k)_p'(u_l)_p'}$$
$$\overline{(u_i)_w'(u_j)_w'(u_k)_w'}=a_{il}\,a_{jm}\,a_{kn}\,\overline{(u_l)_p'(u_m)_p'(u_n)_p'}$$

where $a_{11}=1$, $a_{12}=0$, $a_{13}=0$, $a_{21}=0$, $a_{22}=\cos\theta_r$, $a_{23}=\sin\theta_r$, $a_{31}=0$, $a_{32}=-\sin\theta_r$, $a_{33}=\cos\theta_r$, and θ_r is the roll angle (0° for position 1, 45° for position 2, etc.). Estimates and correction of errors due to the assumption that the instantaneous velocity at both wires is the same, and that $w_w=0$, can then be made.

2.1 Gradient errors

We shall consider first the error incurred when the instantaneous velocity vector is different at the two wires due to gradients normal to the plane of the wire, assuming for now that $w_w=0$. The analysis is similar to that of Hirota et al. (1988). Let us define the measured (suffix m) velocities as the velocities calculated on the assumption that $\Delta=0$. If the velocities and their gradients are referred to $z_w=0$, and a locally linear variation of velocity is assumed, then the effec-

tive cooling velocities are:

$$\frac{1}{\sqrt{2}}(u_{wm}+v_{wm})=\frac{1}{\sqrt{2}}(u_w+v_w)-\frac{\Delta}{2\sqrt{2}}\frac{\partial(u_w+v_w)}{\partial z_w} \text{ for wire 1;}$$

$$\frac{1}{\sqrt{2}}(u_{wm}-v_{wm})=\frac{1}{\sqrt{2}}(u_w-v_w)+\frac{\Delta}{2\sqrt{2}}\frac{\partial(u_w-v_w)}{\partial z_w} \text{ for wire 2.}$$

Solving separately for u_{wm} and v_{wm} we get:

$$u_{wm}=u_w-\frac{\Delta}{2}\frac{\partial v_w}{\partial z_w};$$

$$v_{wm}=v_w-\frac{\Delta}{2}\frac{\partial u_w}{\partial z_w}.$$

Then, forming the mean velocities and Reynolds stresses in wire axes (neglecting terms of order Δ^2):

$$\overline{u_{wm}}=\overline{u_w}-\frac{\Delta}{2}\frac{\partial\overline{v_w}}{\partial z_w} \tag{3}$$

$$\overline{v_{wm}}=\overline{v_w}-\frac{\Delta}{2}\frac{\partial\overline{u_w}}{\partial z_w}$$

$$\overline{u'^2_{wm}}=\overline{u'^2_w}-\Delta\frac{\overline{u'_w\,\partial v'_w}}{\partial z_w}$$

$$\overline{u'_{wm}\,v'_{wm}}=\overline{u'_w\,v'_w}-\frac{\Delta}{4}\frac{\partial\overline{(u'^2_w+v'^2_w)}}{\partial z_w}$$

$$\overline{v'^2_{wm}}=\overline{v'^2_w}-\Delta\frac{\overline{v'_w\,\partial u'_w}}{\partial z_w}$$

The error terms in the measured quantities are the terms of order Δ on the right hand side of Eq. (3). These equations can then be transformed to probe axes using Eq. (2) and the following tensor relations:

$$\frac{\partial\overline{(u_i)_w}}{\partial(x_j)_w}=a_{ik}\,a_{jl}\frac{\partial\overline{(u_k)_p}}{\partial(x_l)_p} \tag{4}$$

$$\frac{\overline{(u_i)_w\,\partial(u_j)_w}}{\partial(x_k)_w}=a_{il}\,a_{jm}\,a_{kn}\frac{\overline{(u_l)_p\,\partial(u_m)_p}}{\partial(x_n)_p}$$

The results from the different roll positions are then substituted into the right-hand-side of Eq. (1) to obtain expressions in probe axes for the errors in the mean velocities and Reynolds stresses.

The gradient error terms in the equations for $\overline{u_{pm}}$, $\overline{v_{pm}}$, and $\overline{w_{pm}}$ are

$$\frac{\Delta}{4}\left(\frac{\partial\overline{w_p}}{\partial y_p}-\frac{\partial\overline{v_p}}{\partial z_p}\right),\ -\frac{\Delta}{2}\frac{\partial\overline{u_p}}{\partial z_p},\ \frac{\Delta}{2}\frac{\partial\overline{u_p}}{\partial y_p}$$

(the error defined in the sense: suffix m value = true value + error). The error terms consist of derivatives with respect to y_p or z_p of mean velocity. The gradient error terms in $\overline{u'_{pm}\,v'_{pm}}$ and $\overline{u'_{pm}\,w'_{pm}}$ are

$$-\frac{\Delta}{4}\left(\frac{\partial\overline{(u'^2_p+v'^2_p)}}{\partial z_p}\right) \text{ and } \frac{\Delta}{4}\left(\frac{\partial\overline{(u'^2_p+w'^2_p)}}{\partial y_p}\right),$$

and consist of derivatives of Reynolds normal stresses. If data are obtained at a number of points in space, these errors can be estimated by direct differentiation of the data and a correction applied. The errors in $\overline{u'^2_{pm}}$, $\overline{v'^2_{pm}}$ and $\overline{w'^2_{pm}}$ are

$$\frac{\Delta}{2}\left(\frac{\overline{u'_p\,\partial w'_p}}{\partial y_p}-\frac{\overline{(u'_p\,\partial v'_p)}}{\partial z_p}\right),\ -\Delta\frac{\overline{v'_p\,\partial u'_p}}{\partial z_p}, \text{ and } \Delta\frac{\overline{w'_p\,\partial u'_p}}{\partial y_p},$$

and cannot be determined from the measurements available. However, these errors are zero by symmetry in a 2-D mean flow. Measurements by Hirota et al. (1988) have shown that for the turbulent flow in a square duct these errors are small everywhere. In general, it appears that the errors in $\overline{u'^2_{pm}}$, $\overline{v'^2_{pm}}$ and $\overline{w'^2_{pm}}$, as a percentage of the quantity being measured, are much smaller than for $\overline{u'_{pm}\,v'_{pm}}$, or $\overline{u'_{pm}\,w'_{pm}}$. The error in the equation for $\overline{v'_{pm}\,w'_{pm}}$ is

$$\frac{\Delta}{2}\left(\frac{\overline{v'_p\,\partial u'_p}}{\partial y_p}-\frac{\overline{(w'_p\,\partial u'_p)}}{\partial z_p}\right),$$

and cannot be estimated either, although experimental results discussed in Sect. 3 suggest it also may be small. It should be remembered that $\overline{v'_{pm}\,w'_{pm}}$ is already a rather uncertain quantity since it is obtained as the difference between two relatively large, experimentally determined quantities.

2.2 High turbulence errors

Let us consider now the effect of the assumption that $w_w=0$. Since we shall be finding the first term in a series expansion of the error, it is acceptable to assume $\Delta=0$ for this analysis. In flows with both high turbulence levels and significant gradients, errors from the two sources will be additive. If the suffix m now refers to those quantities determined assuming $w_w=0$, then the effective cooling velocity for wire 1 is:

$$\frac{1}{\sqrt{2}}(u_{wm}+v_{wm})=\sqrt{\tfrac{1}{2}(u_w+v_w)^2+w_w^2};$$

while the effective cooling velocity for wire 2 is:

$$\frac{1}{\sqrt{2}}(u_{wm}-v_{wm})=\sqrt{\tfrac{1}{2}(u_w-v_w)^2+w_w^2}.$$

Following the analysis of, for example, Bruun (1972), we perform a series expansion for u_{wm} and v_{wm} assuming v_w, $w_w\ll u_w$, getting:

$$u_{wm}+v_{wm}=(u_w+v_w)\left(1+\frac{w_w^2}{(u_w+v_w)^2}+\mathbb{O}(4)\right)$$

$$u_{wm}-v_{wm}=(u_w-v_w)\left(1+\frac{w_w^2}{(u_w-v_w)^2}+\mathbb{O}(4)\right);$$

and solving for u_{wm} and v_{wm}:

$$u_{wm}=u_w\left(1+\frac{w_w^2}{(u_w^2-v_w^2)}+\mathbb{O}(4)\right)$$

$$v_{wm}=v_w\left(1-\frac{w_w^2}{(u_w^2-v_w^2)}+\mathbb{O}(4)\right)$$

The mean velocity and Reynolds stresses are calculated assuming u'_w, v'_w, $w'_w \ll \bar{u}_w$, and $\bar{v}_w$, $\bar{w}_w = 0$:

$$\bar{u}_{wm} = \bar{u}_w \left(1 + \frac{\overline{w'^2_w}}{\bar{u}^2_w} + \mathbb{O}(3)\right) \tag{5}$$

$$\bar{v}_{wm} = \bar{v}_w - \frac{\overline{v'_w w'^2_w}}{\bar{u}^2_w} + \bar{u}_w \, \mathbb{O}(4)$$

$$\overline{u'^2_{wm}} = \overline{u'^2_w} + 2\frac{\overline{u'_w w'^2_w}}{\bar{u}_w} + \bar{u}^2_w \, \mathbb{O}(4)$$

$$\overline{v'^2_{wm}} = \overline{v'^2_w} + \bar{u}^2_w \, \mathbb{O}(4)$$

$$\overline{u'_{wm} v'_{wm}} = \overline{u'_w v'_w} + \frac{\overline{v'_w w'^2_w}}{\bar{u}_w} + \bar{u}^2_w \, \mathbb{O}(4)$$

The error in mean velocity or Reynolds stress which results from assuming that $w_w = 0$ is thus the second term on the right-hand-side of Eq. (5). The assumption in obtaining the error that $\bar{v}_w$, $\bar{w}_w = 0$ is a good one in the experiment we shall describe where the probe is accurately aligned with the mean flow direction. It would however be a simple matter to generalize the analysis to non-zero $\bar{v}_w$, $\bar{w}_w$ and thereby correct for probe misalignment. In the present technique, where all components of mean velocity, Reynolds stresses, and triple products at a given point are measured, the error terms for the mean velocity and the Reynolds stresses can be evaluated explicitly. Equation (5) are transformed from the wire to the probe axes using Eq. (2) and are then substituted into the right-hand-side of Eq. (1) to obtain expressions for the errors in the mean velocities and the Reynolds stresses. The resultant errors in $\bar{u}_{pm}$, $\bar{v}_{pm}$, $\bar{w}_{pm}$, $\overline{u'^2_{pm}}$, $\overline{v'^2_{pm}}$, $\overline{w'^2_{pm}}$, $\overline{u'_{pm} v'_{pm}}$, $\overline{u'_{pm} w'_{pm}}$, and $\overline{v'_{pm} w'_{pm}}$ respectively are:

$$\frac{1}{2\bar{u}_p}(\overline{v'^2_p} + \overline{w'^2_p}); \; -\frac{1}{\bar{u}^2_p}\overline{v'_p w'^2_p}; \; -\frac{1}{\bar{u}^2_p}\overline{v'^2_p w'_p}; \; \frac{1}{\bar{u}_p}(\overline{u'_p v'^2_p} + \overline{u'_p w'^2_p});$$

zero; zero; $\dfrac{\overline{v'_p w'^2_p}}{\bar{u}_p}$; $\dfrac{\overline{v'^2_p w'_p}}{\bar{u}_p}$; and zero.

Note that the error terms in $\overline{v'^2_{pm}}$, $\overline{w'^2_{pm}}$, and $\overline{v'_{pm} w'_{pm}}$, which are zero to the order of accuracy to which we are working, actually involve quadruple and higher order products.

3 Experiment

As part of the study of vortex/boundary-layer interactions described by Cutler and Bradshaw (1987, 1989), extensive measurements were obtained using the technique described above. Probes were calibrated in the free stream of the tunnel in which the experiments were conducted with the vortex generator absent. The dependence of bridge voltage on effective cooling velocity was least-squares fitted to a King's law function with the exponent a parameter of the fit. The effective wire angles were determined by a yaw calibration. Data acquisition and real-time data analysis were performed using a microcomputer with external analog-to-digital converter and sample-and-hold unit. Probe manipulations were performed by a traversing mechanism similar to that described by Shayesteh and Bradshaw (1987) which provided motorized linear, yaw, pitch, and roll movements. The mechanism was designed such that the center of the probe measuring volume remained fixed during yaw, pitch, and roll. During data acquisition, the probe roll axis was aligned with the mean flow to within a degree at each point in the flow. Data acquisition was then as described previously, with mean velocity, Reynolds stress, and triple product data acquired in each of four positions in roll, and combined to give results in probe axes.

During later analysis of the results, the data were transformed from probe to tunnel axes and the error corrections described above were applied. The transformation was similar to the transformation from the probe to the wire axes. We used Eq. (2), modified by dropping the suffix w from the left-hand-side and replacing the tensor a_{ij} with the tensor b_{ij} on the right, where: $b_{11} = \cos\theta_z \cos\theta_y$, $b_{12} = -\sin\theta_z \cos\theta_y$, $b_{13} = \sin\theta_y$, $b_{21} = \sin\theta_z$, $b_{22} = \cos\theta_z$, $b_{23} = 0$, $b_{31} = -\cos\theta_z \sin\theta_y$, $b_{32} = \sin\theta_z \sin\theta_y$, and $b_{33} = \cos\theta_y$. These transformation equations are tedious to evaluate if written in long form, but it is a simple matter to evaluate them for particular numerical values of the data by using DO loops in the data analysis program to perform the summations implied by the repeated indices.

In the experiments of Cutler and Bradshaw (1987, 1989) a pair of counter-rotating stream-wise vortices was generated by a 76° delta wing at an angle of attack, and the vortices interacted with the boundary layer developing on a flat test plate mounted downstream. The common flow between the vortices was towards the surface of the plate so that the boundary layer in this region, although fully turbulent, was diverging and relatively thin. Two cases were studied in detail which differed only in the height above the plate at which the vortices were generated. Figure 3 is a contour and arrow plot showing some of the Reynolds stress and triple product data for Case 2, at $x = 1778$ mm from the leading edge of the plate. The contours are of constant turbulent kinetic energy ($\frac{1}{2}\overline{q'^2} = \frac{1}{2}(\overline{u'^2} + \overline{v'^2} + \overline{w'^2})$), and the arrows are of the diffusion velocity

$$(V_q = (\overline{v'\,u'^2} + \overline{v'^3} + \overline{v'\,w'^2})/\overline{q'^2},\; W_q = (\overline{w'\,u'^2} + \overline{w'\,v'^2} + \overline{w'^3})/\overline{q'^2}).$$

The results are non-dimensionalized on U_{ref}, the nominal free stream velocity. The triple products have been plotted in this way to show the lateral diffusion of the turbulent kinetic energy. The arrows have their base at the y, z position of the data, and the displacement of the arrow is such that $\Delta y/s = V_q/U_{\text{ref}}$ and $\Delta z/s = W_q/U_{\text{ref}}$ (the references length s is 267 mm). Only a fraction of the data used in generating the contours has been plotted as vectors, and vectors have not been plotted where $\overline{q'^2}/U^2_{\text{ref}} < 0.0001$. It is seen that the data are smooth and should be amenable to numerical differentiation. The somewhat irregular appearance of the vortex core can be attributed to an insufficient number of points in the grid and the manner in which the contour-plotting algorithm interpolates between the points.

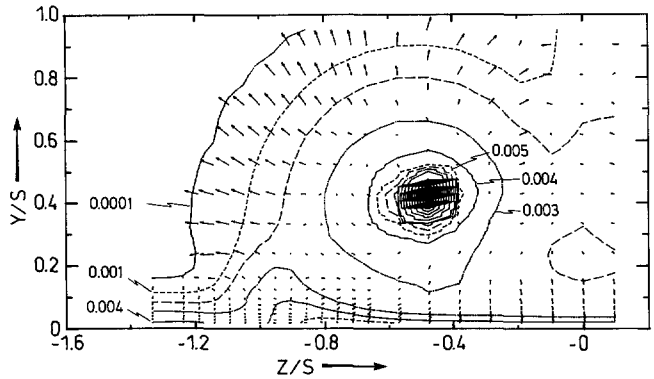

Fig. 3. Contours of turbulent kinetic energy and vectors of diffusion velocity for Case 2 of Cutler and Bradshaw (1987, 1989), at x = 1778 mm

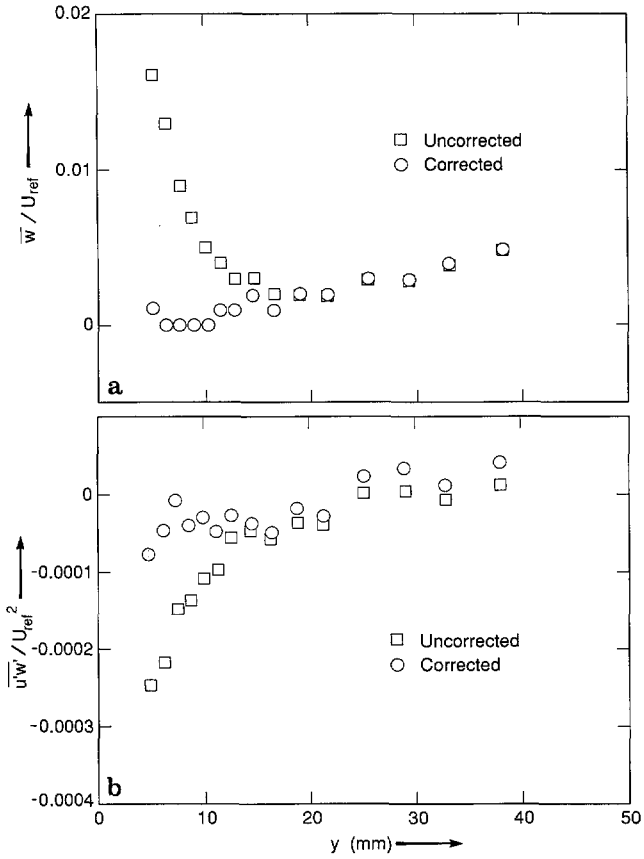

Fig. 4 a and b. The effect of the gradient correction on the data at x = 1778 mm, at the plane of symmetry (z = 0): **a** $\overline{w}$; **b** $\overline{u'w'}$

Initially, no error corrections were applied, and it was noticed that hot-wire measurements of $\overline{w}$ and $\overline{u'w'}$ were consistently non-zero close to the wall at the plane of symmetry (three-hole pitot probe yaw meter measurements confirmed that the mean flow was symmetrical). Measurements of other velocity components and Reynolds stresses were, however, plausible, including $\overline{v'w'}$ which was very close to zero as expected. It seemed probable that these experimental errors could be attributed to the steep gradients of mean velocity and Reynolds stresses in the inner part of the boundary layer. As previously shown, such errors can be corrected by use of mean velocity and Reynolds stress data. Corrections for the errors in $\overline{u}_p$, $\overline{v}_p$, $\overline{w}_p$, $\overline{u'_p v'_p}$, and $\overline{u'_p w'_p}$ were applied in a plane of data. The errors in mean velocity were found by first obtaining the nine terms of the second order tensor $\partial\overline{u_i}/\partial x_j$ in tunnel axes, assuming the $\partial/\partial x$ terms to be zero and $\Delta = 0$, and transforming the tensor to probe axes. The mean velocity errors were then evaluated and transformed back to the tunnel axes to be applied as a correction to the mean velocity data. The error in the Reynolds stresses were found by first obtaining the terms of the third order tensor $\partial\overline{u'_i u'_j}/\partial x_k$ in tunnel axes, then transforming these to the probe axes. The errors in $\overline{u'_p v'_p}$, and $\overline{u'_p w'_p}$ were evaluated while the errors in $\overline{u'^2_p}$, $\overline{v'^2_p}$, $\overline{w'^2_p}$, and $\overline{v'_p w'_p}$ were assumed to be zero for reasons discussed previously. The error tensor was then transformed back to tunnel axes, and applied as a correction to the Reynolds stresses.

Results of these corrections are shown in Fig. 4a, b for Case 2 of Cutler and Bradshaw (1987, 1989) at the plane of symmetry ($z = 0$), at $x = 1778$ mm. The Reynolds number of the boundary layer based on momentum thickness and local edge velocity is 1050 and the 99.5% thickness is about 16 mm. The probe, which is constructed of 0.005 mm diameter platinum core Wollaston wires, has an etched active length of 0.8 mm and a wire spacing (Δ) of 1.6 mm. The effective wire angles relative to the roll axis were between 45° and 48°. It is seen that the correction in $\overline{w}$ and $\overline{u'w'}$ in the region near the wall ($y/\Delta < 10$) is substantial, ≤ 0.015 in $\overline{w}/U_{ref}$, and ≤ 0.0002 in $\overline{u'w'}/U_{ref}^2$. No yaw meter measurements were made at $z = 0$, but a linear interpolation of the results at $z = -25.4$ mm and $z = 25.4$ mm to $z = 0$ indicate a smooth variation of $\overline{w}/U_{ref}$ from -0.0006 ($y = 0.6$ mm) to -0.0017 ($y = 25.4$ mm). Corrected hot-wire results agree with the yaw meter results much better than the uncorrected results. The slight discrepancy at the edge of the boundary layer (< 0.004 in $\overline{w}/U_{ref}$) is consistent with normal calibration errors. The corrections in $\overline{u}$, $\overline{v}$, $\overline{u'^2}$, $\overline{v'^2}$, $\overline{w'^2}$, $\overline{u'v'}$, and $\overline{v'w'}$ were relatively small, as expected. The magnitudes of the errors indicated by Fig. 4 are typical of the gradient errors encountered in the boundary layer region of the vortex/boundary layer interactions we studied. The effect of gradient corrections in the vortex core could not be determined accurately since our data was too sparse there to allow us to determine the derivatives accurately. However, velocity gradients appeared to be very steep at the center of the vortex, suggesting that the gradient errors were substantial.

The high turbulence errors were calculated for Case 2 of Cutler and Bradshaw (1987, 1989) at $x = 1778$ mm. They were relatively small in the boundary layer region: $\overline{u}$ was $< 0.5\%$ high; errors in $\overline{v}$ and $\overline{w}$ were negligible; $\overline{u'^2}$ was $< 1\%$ low; errors in $\overline{v'^2}$ and $\overline{w'^2}$ were negligible; $\overline{u'v'}$ was $< 1.5\%$ low; errors in $\overline{u'w'}/U_{ref}^2$ were less than $\pm 2 \times 10^{-5}$; and errors were negligible in $\overline{v'w'}$ (percentages calculated on the basis

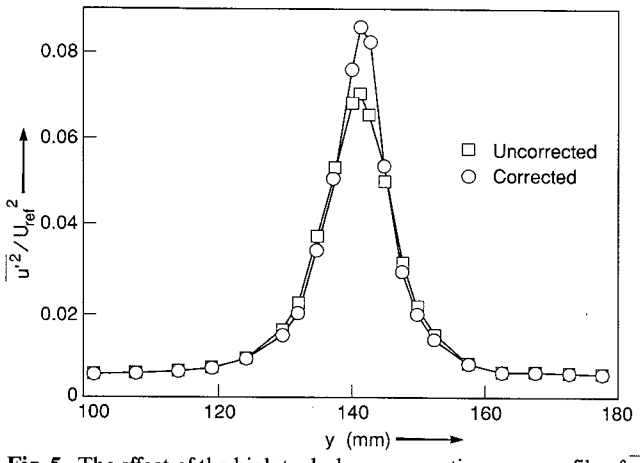

Fig. 5. The effect of the high turbulence correction on a profile of $\overline{u'^2}$ through the center of the vortex at x = 864 mm, z = −108 mm

of local values). However, close to the center of the vortices, where $\sqrt{\overline{u'^2}}/U_{ref} \leq 0.27$, the high turbulence errors were much larger. Figure 5 shows the effect of the correction on a profile of $\overline{u'^2}$ at $x = 864$ mm, $z = -108$ mm, which passed through the center of a vortex. We found that $\overline{u}$ was $< 8\%$ high; errors in $\overline{v}/U_{ref}$ and $\overline{w}/U_{ref}$ were $< \pm 0.03$; $\overline{u'^2}$ was $< 25\%$ low; $\overline{v'^2}$ and $\overline{w'^2}$ were $< 15\%$ low; errors in $\overline{u'v'}/U_{ref}^2$ and $\overline{u'w'}/U_{ref}^2$ were $< \pm 0.01$; and errors in $\overline{v'w'}/U_{ref}^2$ were smaller. High turbulence error corrections were not applied by Cutler and Bradshaw (1987, 1989) because these corrections were small, except near the center of the vortex where the gradient errors were also significant but could not be accurately determined.

4 Conclusions

A crossed hot-wire technique for the measurement of all components of mean velocity, Reynolds stress, and triple products in a complex turbulent flow has been described. The accuracy of the assumption, usually implicit in the use of crossed hot-wire anemometers, that the instantaneous velocity is uniform over the volume defined by the active portion of the two wires, was examined. The magnitude of the errors resulting from this assumption was found to be significant (≤ 0.015 in $\overline{w}/U_{ref}$ and ≤ 0.0002 in $\overline{u'w'}/U_{ref}^2$) close to the wall ($y/\Delta < 10$) in the diverging boundary layer beneath a vortex pair with common flow downwards. A proposed correction brings the results at the plane of symmetry of the flow into line with what was expected on the basis of yaw meter measurement and symmetry arguments. High turbulence errors were found to be small, except near the cores of the vortices where $\sqrt{\overline{u'^2}}/U_{ref} \leq 0.27$ and the errors were large.

References

Bradshaw, P. 1971: An Introduction to turbulence and its measurements, Pergamon Press

Bruun, H. H. 1972: Hot wire data corrections in low and high turbulence intensity flows, J. Phys. E.: Sci. Instrum. 5: 812–818

Cutler, A. D., and Bradshaw, P. 1987: Vortex/boundary-layer interactions, I. C. TN 87–102 (2 Vols.), Imperial College, London

Cutler, A. D., and Bradshaw, P. 1989: Vortex/boundary-layer interactions, AIAA Paper 89–0083

Hirota, M., Fujita, H., and Yokosawa, H. 1988: Influences of velocity gradient on hot-wire anemometry with an X-wire probe, J. Phys. E: Sci. Instrum. 21, 1077–1084

Shayesteh, M. V., and Bradshaw, P. 1987: Microcomputer-controlled traverse gear for three-dimensional flow explorations. J. Phys. E: Sci. Instrum. 20, 320–322

Received December 24, 1990